

Cell-Free Massive MIMO with Underlaid D2D Communications and Low Resolution ADCs

Hamed Masoumi, Mohammad Javad Emadi, and Stefano Buzzi

Abstract

In this article, we investigate uplink transmission of a cell-free massive multiple-input multiple-output (CF-mMIMO) system, underlaid with device-to-device (D2D) communications, and assuming that access points (APs) are equipped with low resolution analog-to-digital converters (ADCs). D2D user equipments (DUEs) are assumed to communicate in the same time-frequency resources as the CF-mMIMO user equipments (CFUEs). We derive closed-form expressions for achievable rates of both types of users, with perfect and imperfect channel state information. A set of orthogonal pilot sequences is reused among all the users to enable channel estimation. Then, greedy and graph coloring-based algorithms are employed to reduce pilot contamination. Furthermore, in order to control interference and improve the performance, two power control strategies are considered; the former aims at maximizing CFUEs' sum spectral efficiency (SE) subject to quality of service constraints on DUEs, while the latter maximizes weighted product of CFUEs' and DUEs' signal-to-interference-plus-noise-ratios (SINRs). For both the optimization problems, a solution based on geometric programming (GP) is developed. Finally, numerical results are provided to highlight the system performance and to show the improvements granted by the use of the proposed pilot assignment algorithms and power allocation solution, compared with the random pilot assignment and full power transmission case.

Index Terms—Cell-free massive MIMO, device to device communications, low resolution ADC, spectral efficiency, uplink data transmission.

H. Masoumi and M. J. Emadi are with the Department of Electrical Engineering, Amirkabir University of Technology (Tehran Polytechnic), Tehran, Iran (e-mails: {hamed_masoomy, mj.emadi}@aut.ac.ir). S. Buzzi is with the Department of Electrical and Information Engineering, University of Cassino and Southern Latium, Cassino, Italy, and with Consorzio Nazionale Interuniversitario per le Telecomunicazioni (CNIT), Parma, Italy (email: buzzi@unicas.it).

I. INTRODUCTION

NUMEROUS solutions, so far, have been introduced to meet demands of the ever growing number of connected devices in wireless network for higher quality of service (QoS) and, among these, two key solutions are cell-free massive MIMO architectures and device to device communications. CF-mMIMO, a promising solution for beyond fifth generation of wireless networks [1], inherits the benefits of both mMIMO systems and networked MIMO systems to serve all users with higher spectral/energy efficiency (SE/EE) [2], [3]. In CF-mMIMO, a large number of distributed antennas or APs are deployed in the coverage area to create macro diversity and to provide increased performance uniformly across users. In addition, D2D communications, which is envisioned as a potential enabler of extreme network densification for the sixth generation of wireless networks [4], allows users in close proximity to directly communicate with each other by reusing the locally available spectrum and increase the system SE [5]. Hence, by underlaying D2D users in a CF-mMIMO deployment it is possible to serve even more users, to greatly improve the overall SE of the system, and to reduce the communication delay by skipping the mobile infrastructure [6]. However, the interference between the CF-mMIMO users and D2D users is an unavoidable price to pay, and is to be properly managed.

A. CF-mMIMO Related Works

Primary groundbreaking works on CF-mMIMO started with the seminal papers [2] and [3], which revealed its potential with respect to classical network deployments. The follow-up studies considered various aspects of CF-mMIMO, including its performance with different approaches [7]–[14], under different non-ideality circumstances [15]–[19], and its functioning in combination with other technologies [20]–[27]. To be specific, [7] studies a user-centric approach along with resource allocation strategies for uplink and downlink data rates and it shows tangible performance improvements compared to the cell-free scenario. In [8], a comprehensive investigation is conducted on the performance of different levels of cooperation among APs, and it turns out that with global or local minimum mean square error (MMSE) CF-mMIMO outperforms the classical cellular counterpart significantly. From EE perspectives, assuming per AP power and per user SE constraints, [9] maximizes total EE of downlink transmission, while [10] minimizes

total downlink power consumption by joint power allocation and active AP selection for load balancing. In [11], authors present a pilot power allocation problem aimed at optimizing the channel estimation normalized total mean square error, with random pilot assignment and largest large-scale fading-based AP selection scheme. [12] exploits the Hungarian algorithm for pilot allocation in CF-mMIMO to improve uplink and downlink SEs. Uplink SE of the CF-mMIMO using zero-forcing (ZF) detector with perfect and imperfect channel state information (CSI) is investigated in [13] and several asymptotic results are derived. In order to achieve green CF-mMIMO, [14] explores multiple heuristic AP on/off strategies for optimizing uplink and downlink energy efficiency of the system based on number and location of the active users. Moreover, [15] investigates the effect of low resolution analog-to-digital converters (ADCs) in both APs and user equipment (UEs) for the downlink of CF-mMIMO and presents a max-min power control. Also, orthogonal pilots are used for channel estimation. In [16], uplink SE of a CF-mMIMO system with multiple antenna UEs and APs and low resolution ADCs at the APs are studied. Uplink transmission of CF-mMIMO with limited fronthaul links and max-min fairness power allocation is addressed by [17]. In [18], the uplink of CF-mMIMO with limited fronthaul capacity and hardware impairments, i.e. aggregate effects of different non-idealities, at both APs and UEs are considered and the sum rate maximization problem is investigated.

In parallel, many researchers studied CF-mMIMO in coexistence with other novel technologies to investigate the interplay between CF-mMIMO and those technologies. The total energy efficiency for the uplink and downlink of both a CF-mMIMO system and a user-centric system in millimeter wave frequency bands is maximized in [20], assuming hybrid beamforming. In a spectrum sharing scenario, the downlink performance of CF-mMIMO system as a secondary network that is underlaid below a co-located mMIMO system with non-orthogonal multiple access (NOMA) technique is scrutinized in [21]. [22] inspects the support for unmanned aerial vehicles as well as ground users in CF-mMIMO networks for the uplink and downlink transmissions along with max-min power allocation. Moreover, SE of CF-mMIMO with full-duplex APs, ZF/regularized-ZF combining is analyzed in [23], where a user scheduling scheme is also presented. Furthermore, authors of [24] examine an adaptive mode switching between NOMA

and orthogonal multiple access for the downlink of CF-mMIMO with max-min power control. A deep learning approach has been recently employed for sum SE maximization by controlling transmit power of users in a fronthaul limited CF-mMIMO [25]. Finally, in [26] and [27] authors explore the application of deep learning for channel estimation in millimeter wave bands and mobile edge computing in CF-mMIMO, respectively.

B. D2D Related Works

Due to the increasing number of devices and the rise of machine-to-machine applications, the ability of nearby devices to communicate directly in order to improve SE/EE and cut down delay and power consumption has gained considerable research interests [28]–[36]. In [28], the uplink of a single-cell mMIMO network with underlaid D2D users is studied, the channel of each D2D pair is estimated using pilots which are orthogonal with the pilots of cellular users and are reused among D2D pairs. A graph coloring strategy is applied for pilot assignment, and an optimization problem for minimizing sum power consumption of D2D transmitters subject to QoS for cellular users is proposed. Authors in [29] assume the similar setting as [28], with the exception that each cellular user transmits in different resource blocks, and D2D users reuse these resources creating interference. Then, instantaneous EE of D2D users subject to QoS constraints for cellular users is maximized. For a similar setting, the sum SE of D2D users is maximized in [30], with cellular users assumed to operate in downlink mode. [31] addresses open-loop power control for the uplink of multi-cell mMIMO systems with underlaid D2D pairs and without considering channel estimation or pilot transmission. [32] studies the sum SE maximization of D2D users subject to QoS constraints for cellular users in the uplink of single cell mMIMO, with channel estimation using pilots that are reused among D2D pairs but orthogonal with cellular users. In [34], uplink multi-cell mMIMO system with underlaid D2D pairs is investigated; in particular, asymptotic and non-asymptotic SE of cellular and D2D users with perfect and imperfect CSI using orthogonal pilots and without power allocation is analysed. For D2D-based vehicle-to-vehicle (V2V) pairs that are underlaid in the uplink of a single-cell mMIMO system, the SE of the V2V users and cellular users with perfect CSI and using ZF and maximum ratio combining are derived in [35]. Next, a transmit power optimization problem

with the objective of maximizing sum SE of V2V users subject to QoS for cellular users is proposed. In [36], uplink of multi-cell mMIMO system with underlaid D2D users is considered. Also, orthogonal pilots are used for channel estimation, where MRC and ZF are used for symbol detection and to derive the SE of both cellular UEs and D2D users. Finally, max-min fairness of the users and maximization of the product of SINRs are addressed.

C. Contribution

We consider uplink transmission in a CF-mMIMO network with underlaid D2D communications. To the best of our knowledge, the coexistence of these two technologies has not yet been investigated throughout the literature. This coexistence not only can help to significantly improve the SE of the system by reusing the available time-frequency resources, but it can also improve the EE for users that can establish a short-range link via D2D communications. Additionally, using low resolution ADC modules at the APs is essential in order to cost-efficiently deploy a vast number of APs throughout the coverage area. Accordingly, low resolution ADCs at the APs are also considered in this work. To manage the mutual interference between DUEs and CFUEs sharing the same time-frequency resources, we present and solve two optimization problems: the former maximizes the SE of CFUEs with QoS constraints on DUEs SE, while the latter maximizes the weighted product of SINRs of DUEs and CFUEs. We also assume that there is a limited number of orthogonal pilots which are reused among DUEs and CFUEs for channel estimation, and thus, two pilot assignment algorithms are considered to manage pilot contamination. Our contributions can be thus summarized as follows.

- For the uplink of CF-mMIMO with *underlaid D2D users* and *low resolution ADCs* at the APs, *closed-form SE* formulas for both CFUEs and DUEs with perfect and imperfect CSI are derived.
- A limited number of orthogonal pilots is *reused* among all the users, and MMSE channel estimation is performed for estimating the channels. Also, a *greedy-based algorithm* for CFUEs and a *graph coloring-based algorithm* for DUEs are adopted for pilot assignment to reduce the pilot contamination.

- *Two power allocations* are investigated to further improve the system performance. In the former, sum SE of CFUEs are maximized subject to QoS for DUEs and maximum transmit power. In the latter, the weighted product of SINRs of CFUEs and DUEs is maximized subject to maximum transmit power of the users. For both problems a GP-based solution is presented to obtain the optimal power control coefficients.
- Finally, numerical results are provided to evaluate the performance of the proposed resource allocation problems in the considered scenario.

Organization: In the remainder of the article we present the system model in Section II. The performance analysis is carried out in Section III, and pilot assignment and power control are addressed in Section IV. Finally, Section V and VI are devoted to numerical results and conclusions, respectively.

Notation: For matrices and vectors we use boldface uppercase and boldface lowercase letters, respectively. $\mathbf{x} \in \mathbb{C}^{N \times 1}$ denotes a vector in a N -dimensional complex space, δ_{ij} equals 1 for $i = j$ and 0 otherwise. Moreover, $(\cdot)^*$, $(\cdot)^T$ and $(\cdot)^H$ are used for denoting conjugate, transpose and conjugate-transpose operators. Finally, $\mathcal{CN}(0, \sigma^2)$ represents the zero-mean circularly symmetric complex Gaussian (CSCG) distribution with variance σ^2 .

II. SYSTEM MODEL

We consider the uplink of CF-mMIMO system with underlaid D2D communications in which K single-antenna CFUEs communicate with M distributed single-antenna access points; simultaneously, L D2D pairs communicate in the considered system as shown in Fig. 1. Similar to [34] and [32], we assume a single-antenna transmitter, for instance DUE_l^{tx} , and an N -antenna receiver counterpart, i.e. DUE_l^{rx} , for D2D communications¹. Note that $K \ll M$ and all the communications take place in the same time-frequency resource. The time division duplex protocol is used to exploit the channel reciprocity for reducing channel estimation overhead and to make system scalable. Also, APs are assumed to be equipped with low resolution ADCs for deployment cost reduction.

¹Please note that the results can be straightforwardly extended to the full MIMO scenario.

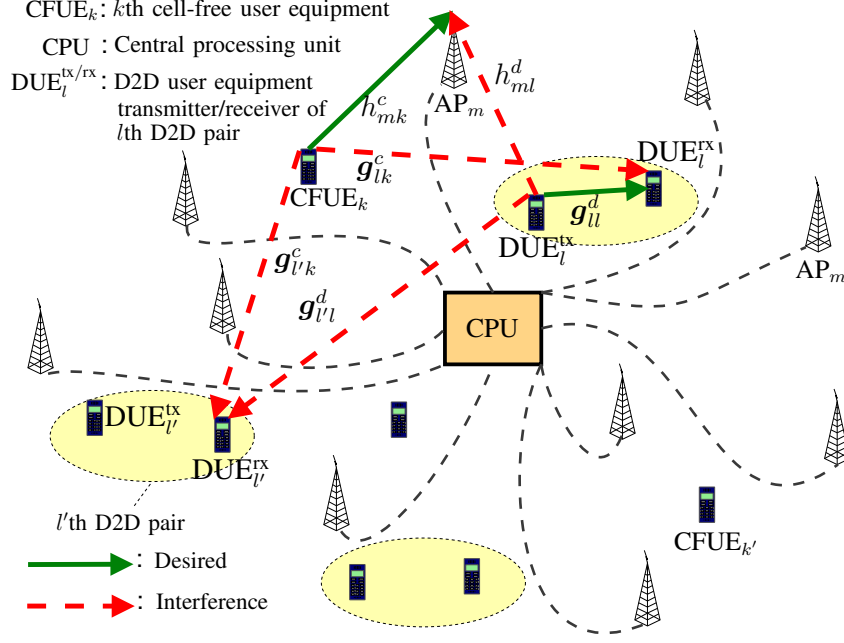


Fig. 1. Cell-free mMIMO with underlaid D2D communications system model.

A. Channel Model

We consider Rayleigh fading channel model which is constant in each coherence interval of length T [samples], and changes independently from one coherence interval to another. The channel between the k th CFUE for $k \in \mathcal{K} = \{1, 2, \dots, K\}$ or the transmitter of l th DUE pair for $l \in \mathcal{L} = \{1, 2, \dots, L\}$ and the m th AP is modeled by $h_{mt_i}^i \sim \mathcal{CN}(0, \beta_{mt_i}^i)$ where $i = c$ identifies CFUE transmitters while $i = d$ identifies DUE transmitters, and $t_c \in \mathcal{K}$, $t_d \in \mathcal{L}$. Moreover, the channel between those transmitters and the receiver of the l' th DUE pair is given by $g_{l't_i}^i \sim \mathcal{CN}(0, \psi_{l't_i}^i \mathbf{I}_N)$, where \mathbf{I}_N is the $N \times N$ identity matrix and $\beta_{mt_i}^i$, $\psi_{l't_i}^i$ account for the large-scale fading coefficients.

B. Modelling Impacts of Low Resolution ADCs

The received baseband signal at the m th AP and at the receiver of l th DUE pair are respectively given by

$$\bar{y}_m^c = \sqrt{\rho^c} \sum_{k=1}^K \sqrt{\eta_k^c} h_{mk}^c s_k^c + \sqrt{\rho^d} \sum_{l'=1}^L \sqrt{\eta_{l'}^d} h_{ml'}^d s_{l'}^d + n_m^c, \quad (1a)$$

TABLE I
VALUES OF ξ FOR $b \in \{1, 2, 3, 4, 5\}$.

b	1	2	3	4	5
ξ	0.6366	0.8825	0.96546	0.990503	0.997501

$$\mathbf{y}_l^d = \sqrt{\rho^c} \sum_{k=1}^K \sqrt{\eta_k^c} \mathbf{g}_{lk}^c s_k^c + \sqrt{\rho^d} \sum_{l'=1}^L \sqrt{\eta_{l'}^d} \mathbf{g}_{ll'}^d s_{l'}^d + \mathbf{n}_l^d, \quad (1b)$$

where $s_{t_i}^i \sim \mathcal{CN}(0, 1)$ is the transmitted information symbol by the t_i th user, which is assumed to be independent and identically distributed (i.i.d) for different users. Furthermore, ρ^i and $\eta_{t_i}^i$ denote the maximum transmit power and the power control coefficient, respectively. Also, $n_m^c \sim \mathcal{CN}(0, N_0)$ is the additive white Gaussian noise (AWGN) at the m th AP and \mathbf{n}_l^d is an $N \times 1$ vector of i.i.d AWGN random variables distributed according to $\mathcal{CN}(0, N_0)$. Since low resolution ADCs are used at the APs, the received signal (1a) for the m th AP is actually written as follows [37]–[40]

$$y_m^c = \xi \bar{y}_m^c + q_m = \xi \sqrt{\rho^c} \sum_{k=1}^K \sqrt{\eta_k^c} h_{mk}^c s_k^c + \xi \sqrt{\rho^d} \sum_{l'=1}^L \sqrt{\eta_{l'}^d} h_{ml'}^d s_{l'}^d + \xi n_m^c + q_m. \quad (2)$$

In (2) we have used the so called additive quantization noise model (AQNM); in particular, q_m accounts for the quantization noise which is uncorrelated with \bar{y}_m and for a non-uniform quantizer has the following variance $Q_m = \mathbb{E}\{q_m^* q_m | \{h_{mt_i}^i\}\}$ [38], [39], [41]; with

$$Q_m = (1 - \xi) \xi \mathbb{E}\{\bar{y}_m^c \bar{y}_m^c | \{h_{mt_i}^i\}\} = (1 - \xi) \xi \left(\rho^c \sum_{k=1}^K \eta_k^c |h_{mk}^c|^2 + \rho^d \sum_{l'=1}^L \eta_{l'}^d |h_{ml'}^d|^2 + N_0 \right). \quad (3)$$

In (3), ξ can be specified in terms of the number of ADC quantization bits b ; for $b > 5$, ξ is computed as $\xi = 1 - \frac{\pi\sqrt{3}}{2} 2^{-2b}$ and for other values of b it can be obtained from Table I [39].

III. PERFORMANCE ANALYSIS

In this section, the uplink achievable rate of the system for the CFUEs and for the DUEs are derived under perfect CSI. Next, imperfect CSI is obtained using uplink channel training and the corresponding achievable data rates are derived.

A. Uplink Achievable Rate with Perfect CSI

1) *Achievable rate of CFUEs:* When perfect CSI is available, using (2) and MRC receiver the following approximation of the transmitted symbol for k th CFUE at the CPU can be derived.

$$\begin{aligned}
 r_k^c &= \sum_{m=1}^M h_{mk}^{c*} y_m^c = \underbrace{\xi \sqrt{\eta_k^c \rho^c} \sum_{m=1}^M |h_{mk}^c|^2 s_k^c}_{\text{DS}_k: \text{desired signal}} + \mathcal{I}_k^c, \\
 \mathcal{I}_k^c &= \underbrace{\xi \sqrt{\rho^c} \sum_{k' \neq k}^K \sqrt{\eta_{k'}^c} \sum_{m=1}^M h_{mk}^{c*} h_{mk'}^c s_{k'}^c}_{\text{ICFUE}_k: \text{interference from CFUEs}} + \underbrace{\xi \sqrt{\rho^d} \sum_{l'=1}^L \sqrt{\eta_{l'}^d} \sum_{m=1}^M h_{mk}^{c*} h_{ml'}^d s_{l'}^d}_{\text{IDUE}_k: \text{interference from DUEs}} + \underbrace{\xi \sum_{m=1}^M h_{mk}^{c*} n_m}_{\text{TN}_k: \text{total noise}} + \underbrace{\sum_{m=1}^M h_{mk}^{c*} q_m}_{\text{QN}_k: \text{quantization noise}},
 \end{aligned} \tag{4}$$

where \mathcal{I}_k^c includes the interference from other CFUEs, DUE transmitters, the channel noise and the quantization noise as the result of deploying low resolution ADCs. It can be shown that for a given channel realization all the terms in (4) are mutually uncorrelated. So, the ergodic achievable rate of the k th CFUE with perfect CSI is expressed as

$$R_k^{\text{CFUEP}} = \mathbb{E} \left\{ \log_2 \left(1 + \frac{|\text{DS}_k|^2}{\text{Var}(\mathcal{I}_k^c)} \right) \right\}, \tag{5}$$

where the superscript P, stands for *perfect* CSI and $\text{Var}(\cdot)$ indicates the variance operator. Given the perfect CSI, the variance of \mathcal{I}_k^c can be written as

$$\begin{aligned}
 \text{Var}(\mathcal{I}_k^c) &= \xi^2 \rho^c \sum_{k' \neq k}^K \eta_{k'}^c \left| \sum_{m=1}^M h_{mk}^{c*} h_{mk'}^c \right|^2 + \xi^2 \rho^d \sum_{l'=1}^L \eta_{l'}^d \left| \sum_{m=1}^M h_{mk}^{c*} h_{ml'}^d \right|^2 + N \xi \sum_{m=1}^M |h_{mk}^c|^2 \\
 &+ (1 - \xi) \xi \left(\rho^c \sum_{k=1}^K \eta_{k'}^c \sum_{m=1}^M |h_{mk}^c|^2 |h_{mk'}^c|^2 + \rho^d \sum_{l'=1}^L \eta_{l'}^d \sum_{m=1}^M |h_{mk}^c|^2 |h_{ml'}^d|^2 \right).
 \end{aligned} \tag{6}$$

Notice that in computing the above variance we also used (3). Next, in order to obtain a *closed-form* expression for the achievable rate, the well-known *use and then forget* (UatF) technique [42] is applied to the statistic (4), resulting in the following expression

$$r_k = \mathbb{E}\{\text{DS}_k\} s_k + \text{BU}_k s_k + \mathcal{I}_k^c, \tag{7}$$

where $\text{BU}_k = \{\text{DS}_k - \mathbb{E}\{\text{DS}_k\}\}$ and stands for beamforming uncertainty. Since all the terms in (7) are also mutually uncorrelated, by considering that the last two interfering terms follow the worst case Gaussian distribution, the achievable rate is given by

$$R_{k,\text{UatF}}^{\text{CFUEp}} = \log_2 \left(1 + \frac{|\mathbb{E}\{\text{DS}_k\}|^2}{\text{Var}(\text{BU}_k) + \text{Var}(\mathcal{I}_k^c)} \right). \quad (8)$$

Theorem 1. *The closed-form achievable rate of k th CFUE with perfect CSI is*

$$R_{k,\text{UatF}}^{\text{CFUEp}} = \log_2 \left(1 + \frac{\xi \eta_k^c \rho^c \left(\sum_{m=1}^M \beta_{mk}^c \right)^2}{\rho^c \sum_{k'=1}^K \eta_{k'}^c \sum_{m=1}^M \beta_{mk}^c \beta_{mk'}^c + \rho^d \sum_{l'=1}^L \eta_{l'}^d \sum_{m=1}^M \beta_{mk}^c \beta_{ml'}^d + (1-\xi) \rho^c \eta_k^c \sum_{m=1}^M \beta_{mk}^{c^2} + N_0 \sum_{m=1}^M \beta_{mk}^c} \right). \quad (9)$$

Proof. See Appendix A. □

2) *Achievable rate of DUEs:* By having perfect CSI, MRC combining technique can be applied at the receiver of the l th D2D pair, i.e. equation (1b), which leads to

$$r_l^d = \underbrace{\mathbf{g}_{ul}^{dH} \mathbf{y}_l^d}_{\text{DS}_k} = \underbrace{\sqrt{\rho^d \eta_l^d} \|\mathbf{g}_{ul}^d\|^2 s_l^d}_{\text{ICFUE}_k} + \underbrace{\sqrt{\rho^c} \sum_{k=1}^K \sqrt{\eta_k^c} \mathbf{g}_{ul}^{dH} \mathbf{g}_{lk}^c s_k^c}_{\text{IDUE}_k} + \underbrace{\sqrt{\rho^d} \sum_{l' \neq l}^L \sqrt{\eta_{l'}^d} \mathbf{g}_{ul}^{dH} \mathbf{g}_{ll'}^d s_{l'}^d}_{\text{IDUE}_k} + \underbrace{\mathbf{g}_{ul}^{dH} \mathbf{n}_l^d}_{\text{TN}_k}, \quad (10)$$

Since for given channel realizations, the interference terms, i.e. ICFUE_k , IDUE_k and TN_k , and the desired signal follow a Gaussian distribution and are mutually independent from one another, the ergodic achievable rate for the receiver of l th D2D pair is derived as

$$R_l^{\text{DUEp}} = \mathbb{E} \left\{ \log_2 \left(1 + \frac{\rho^d \eta_l^d \|\mathbf{g}_{ul}^d\|^4}{\rho^c \sum_{k=1}^K \eta_k^c |\mathbf{g}_{ul}^{dH} \mathbf{g}_{lk}^c|^2 + \rho^d \sum_{l' \neq l}^L \eta_{l'}^d |\mathbf{g}_{ul}^{dH} \mathbf{g}_{ll'}^d|^2 + N_0 \|\mathbf{g}_{ul}^d\|^2} \right) \right\}. \quad (11)$$

To obtain a closed-form expression for the above ergodic rate, by using the Jensen's inequality according to

$$\log \left(1 + \frac{1}{\mathbb{E}\{x\}} \right) \leq \mathbb{E} \left\{ \log \left(1 + \frac{1}{x} \right) \right\}, \quad (12)$$

the following theorem can be stated.

Theorem 2. *The achievable rate of l th DUE with perfect CSI and $N \geq 2$ is*

$$R_{k,apx}^{DUE_p} = \log_2 \left(1 + \frac{\rho^d \eta_l^d \psi_{ll}^d (N-1)}{\rho^c \sum_{k=1}^K \eta_k^c \psi_{lk}^c + \rho^d \sum_{l' \neq l}^L \eta_{l'}^d \psi_{ll'}^d + N_0} \right). \quad (13)$$

Proof. See Appendix B. □

B. Uplink Achievable Rate with Imperfect CSI

In this subsection we first present the uplink channel estimation procedure, and then the achievable data rates of CFUEs and DUEs are derived using the obtained estimates.

1) *Channel Estimation:* For obtaining channel estimates, τ -length orthogonal pilot sequences, denoted by $\Phi = \{\phi_1, \phi_2, \dots, \phi_\tau\}$, are considered, where $\phi_u^H \phi_v = \delta_{uv}$ and $\phi_u \in \mathbb{C}^{\tau \times 1}$, $\{u, v\} = 1, 2, \dots, \tau$. Hence, the channel estimation overhead is $\varsigma = \frac{T-\tau}{T}$. The assigned pilots for CFUE k and DUE l are denoted by $\omega_k \in \Phi$ and $\theta_l \in \Phi$, respectively. Also, the total transmit power and the power control coefficients of the t_i th CFUE or DUE are indicated by ρ_p^i and $\mu_{t_i}^i$, respectively. Thus, the m th AP receives a $\tau \times 1$ vector $\mathbf{y}_{p,m}^c$, and the receiver of the l th D2D pair receives an $N \times \tau$ matrix $\mathbf{Y}_{p,l}^d$ as follows

$$\mathbf{y}_{p,m}^c = \xi \sqrt{\tau \rho_p^c} \sum_{k=1}^K \sqrt{\mu_k^c} h_{mk}^c \omega_k + \xi \sqrt{\tau \rho_p^d} \sum_{l'=1}^L \sqrt{\mu_{l'}^d} h_{ml'}^d \theta_{l'} + \xi \mathbf{n}_{p,m}^c + \mathbf{q}_{p,m}, \quad (14a)$$

$$\mathbf{Y}_{p,l}^d = \sqrt{\tau \rho_p^c} \sum_{k=1}^K \sqrt{\mu_k^c} \mathbf{g}_{lk}^c \omega_k^H + \sqrt{\tau \rho_p^d} \sum_{l'=1}^L \sqrt{\mu_{l'}^d} \mathbf{g}_{ll'}^d \theta_{l'}^H + \mathbf{N}_{p,l}^d. \quad (14b)$$

In the above equations $\mathbf{q}_{p,m}$ is a $\tau \times 1$ quantization noise vector whose covariance matrix is defined as $\mathbf{Q}_{p,m} = (1 - \xi) \xi \mathbb{E} \left\{ \bar{\mathbf{y}}_{p,m}^c \bar{\mathbf{y}}_{p,m}^{cH} \right\}$, with $\bar{\mathbf{y}}_{p,m}^c$ the received signal at the m th AP for the case of infinite resolution ADCs. Furthermore, the $\tau \times 1$ vector $\mathbf{n}_{p,m}^c$ and the $N \times \tau$ matrix $\mathbf{N}_{p,l}^d$ are additive white noises contributions with i.i.d entries distributed according to $\mathcal{CN}(0, N_0)$. After projecting the received signals onto the used pilot sequences the channel between k th CFUE and AP m is estimated using linear minimum mean square error (LMMSE) as follows [43, chapter

7]

$$\hat{h}_{mk}^c = \frac{\sqrt{\tau \rho_p^c \mu_k^c \beta_{mk}^c}}{\tau \rho_p^c \sum_{k'=1}^K \mu_{k'}^c \beta_{mk'}^c |\boldsymbol{\omega}_k^H \boldsymbol{\omega}_{k'}|^2 + \tau \rho_p^d \sum_{l'=1}^L \mu_{l'}^d \beta_{ml'}^d |\boldsymbol{\omega}_k^H \boldsymbol{\theta}_{l'}|^2 + N_0} y_{p,mk}^c = \lambda_{mk}^c y_{p,mk}^c, \quad (15)$$

where $y_{p,mk}^c = \boldsymbol{\omega}_k^H \mathbf{y}_{p,m}^c$ and the variance of the channel estimate is given by $\gamma_{mk}^c = \xi \sqrt{\tau \rho_p^c \mu_k^c \beta_{mk}^c} \lambda_{mk}^c$.

Next, estimates of the D2D channels are obtained from (14b) as follows

$$\hat{\mathbf{g}}_{ll}^d = \frac{\sqrt{\tau \rho_p^d \mu_l^d \psi_{ll}^d}}{\tau \rho_p^c \sum_{k=1}^K \mu_k^c \psi_{lk}^c |\boldsymbol{\omega}_k^H \boldsymbol{\theta}_l|^2 + \tau \rho_p^d \sum_{l'=1}^L \mu_{l'}^d \psi_{ll'}^d |\boldsymbol{\theta}_{l'}^H \boldsymbol{\theta}_l|^2 + N_0} \mathbf{y}_{p,ll}^d = \lambda_{ll}^d \mathbf{y}_{p,ll}^d, \quad (16)$$

where $\mathbf{y}_{p,ll}^d = \mathbf{Y}_{p,l}^d \boldsymbol{\theta}_l$ and $\mathbb{E} \{ \hat{\mathbf{g}}_{ll}^d \hat{\mathbf{g}}_{ll}^{dH} \} = \sqrt{\tau \rho_p^d \mu_l^d \psi_{ll}^d} \lambda_{ll}^d \mathbf{I}_{N \times N} = \gamma_{ll}^d \mathbf{I}_{N \times N}$.

2) *Achievable rate:* In the following, based on the estimated channels and by applying a MRC receiver, the achievable data rate of the CFUEs and DUEs are presented.

Theorem 3. *The closed form achievable data rate for k th CFUE with imperfect CSI is given by*

$$R_{k,UatF}^{CFUEIP} = \varsigma \log_2 \left(1 + \frac{\xi^2 \eta_k^c \rho^c \left(\sum_{m=1}^M \gamma_{mk}^c \right)^2}{\xi \rho^c \sum_{k'=1}^K \eta_{k'}^c \sum_{m=1}^M \gamma_{mk'}^c \beta_{mk'}^c + \xi \rho^d \sum_{l'=1}^L \eta_{l'}^d \sum_{m=1}^M \gamma_{mk'}^d \beta_{ml'}^d + \xi N_0 \sum_{m=1}^M \gamma_{mk} + (1 - \xi^2) \rho^c \eta_k^c \sum_{m=1}^M \gamma_{mk}^2} \right. \\ \left. + \rho^c \sum_{k' \neq k}^K \eta_{k'}^c \sum_{m=1}^M \left(\gamma_{mk}^c \frac{\sqrt{\mu_{k'}^c \beta_{mk'}^c}}{\sqrt{\mu_k^c \beta_{mk}^c}} \right)^2 |\boldsymbol{\omega}_k^H \boldsymbol{\omega}_{k'}|^2 + \rho^d \sum_{l'=1}^L \eta_{l'}^d \sum_{m=1}^M \left(\gamma_{mk}^d \frac{\sqrt{\mu_{l'}^d \beta_{ml'}^d}}{\sqrt{\mu_k^d \beta_{mk}^d}} \right)^2 |\boldsymbol{\omega}_k^H \boldsymbol{\theta}_{l'}|^2 \right) } \quad (17)$$

Sketch of Proof. By applying the UatF technique and following a similar approach as that in the case of perfect CSI, the achievable data rate is derived, as detailed in Appendix C. \square

For deriving the achievable data rate of the l th DUE receiver we write $\mathbf{g}_{ll}^d = \hat{\mathbf{g}}_{ll}^d + \boldsymbol{\varepsilon}_{ll}^d$, where $\boldsymbol{\varepsilon}_{ll}^d$ is the LMMSE estimation error and it is independent from the estimated channel. Thus, the

combined signal using MRC and imperfect CSI is given by

$$\begin{aligned}
 r_l^d = \hat{\mathbf{g}}_{ll}^{dH} \mathbf{y}_l^d = & \underbrace{\sqrt{\rho^d \eta_l^d} \|\hat{\mathbf{g}}_{ll}^d\|^2 s_l^d}_{\text{DS}_k} + \underbrace{\sqrt{\rho^c} \sum_{k=1}^K \sqrt{\eta_k^c} \hat{\mathbf{g}}_{ll}^{dH} \mathbf{g}_{lk}^c s_k^c}_{\text{ICFUE}_k} + \underbrace{\sqrt{\rho^d} \sum_{l' \neq l}^L \sqrt{\eta_{l'}^d} \hat{\mathbf{g}}_{ll}^{dH} \mathbf{g}_{ll'}^d s_{l'}^d}_{\text{IDUE}_k} \\
 & + \underbrace{\hat{\mathbf{g}}_{ll}^{dH} \sqrt{\rho^d \eta_l^d} \boldsymbol{\varepsilon}_{ll}^d s_l^d}_{\text{TEE}_k: \text{ Total Estimation Error}} + \underbrace{\hat{\mathbf{g}}_{ll}^{dH} \mathbf{n}_l^d}_{\text{TN}_k}.
 \end{aligned} \tag{18}$$

Note that $\mathbb{E}\{\boldsymbol{\varepsilon}_{ll}^d \boldsymbol{\varepsilon}_{ll}^{dH}\} = (\psi_{ll}^d - \gamma_{ll}^d) \mathbf{I}_{N \times N}$, and therefore, by treating the interfering terms as an equivalent Gaussian noise, the ergodic rate for the l th DUE is obtained as (19)

$$R_l^{\text{DUEip}} = \varsigma \mathbb{E} \left\{ \log_2 \left(1 + \frac{\rho^d \eta_l^d \|\hat{\mathbf{g}}_{ll}^d\|^4}{\|\hat{\mathbf{g}}_{ll}^d\|^2 \rho^c \sum_{k=1}^K \eta_k^c \psi_{lk}^c + \|\hat{\mathbf{g}}_{ll}^d\|^2 \rho^d \sum_{l' \neq l}^L \eta_{l'}^d \psi_{ll'}^d + \|\hat{\mathbf{g}}_{ll}^d\|^2 \rho^d \eta_l^d (\psi_{ll}^d - \gamma_{ll}^d) + N_0 \|\hat{\mathbf{g}}_{ll}^d\|^2} \right) \right\}. \tag{19}$$

Theorem 4. *The closed form achievable data rate for l th DUE with imperfect CSI is given by*

$$R_{l, \text{apx}}^{\text{DUEip}} = \varsigma \log_2 \left(1 + \frac{\rho^d \eta_l^d \gamma_{ll}^d (N - 1)}{\rho^c \sum_{k=1}^K \eta_k^c \psi_{lk}^c + \rho^d \sum_{l' \neq l}^L \eta_{l'}^d \psi_{ll'}^d + \rho^d \eta_l^d (\psi_{ll}^d - \gamma_{ll}^d) + N_0} \right). \tag{20}$$

Sketch of Proof. By applying (12) in (19) and following a similar approach as that in the case of perfect CSI, the achievable data rate is derived (see Appendix B). \square

IV. PILOT ASSIGNMENT AND POWER ALLOCATION

In this section two pilot assignment strategies are presented in order to control the pilot contamination effect in the training phase and improve the channel estimation quality. Then, two power control optimization problems are formulated to further enhance the performance of the system.

A. Pilot Assignment

As one can recognize from the channel estimates given in (15) and (16), sharing pilots between CFUEs and DUEs introduces the second term in the denominator of (15) and (16), expressing the

Algorithm 1 Greedy-based CFUE pilot allocation (GCPA)

Input: Large-scale fading coefficients $\beta_{mk}^c, \forall \{m, k\}$, set of available orthogonal pilots $\Omega = \{\omega_1, \dots, \omega_{\tau_c}\}$, number of iterations T , iteration index $t = 1$.

I. Iteration t :

I.1. Use (17) and find the following

$$\hat{k} = \arg \min_k R_{k, \text{UatF}}^{\text{CFUE}_{\text{IP}}}.$$

I.2. Choose $\omega_{\hat{k}}$ from the set of CFUE pilots that minimizes following term

$$\omega_{\hat{k}} = \arg \min_{\pi_{\hat{k}} \in \Omega} \sum_{m=1}^M \sum_{k' \neq \hat{k}}^K \mu_{k'}^c \beta_{mk'}^c \left| \pi_{\hat{k}}^H \omega_{k'} \right|^2$$

II. If $t = T$ stop. Otherwise $t = t + 1$ and go to **I**.

Output: The assigned pilots $\omega_k \forall k$.

pilot contamination between DUEs on CFUEs, which degrades the channel estimation quality. To circumvent this drawback, we first remove this coupling by assigning different sets of orthogonal pilots to CFUEs and DUEs, and then we employ established pilot assignment techniques to allocate the pilots among the users. Although in this way the frequency of reusing a certain pilot among CFUEs or DUEs may increase, it permits us to apply modified version of proven pilot assignment techniques, such as greedy [2] and graph coloring-based [44] pilot assignments, to improve the system performance. It is worth to mention that this decoupling will also simplify the rate expressions, e.g. terms that include $\omega_k^H \theta_l$ will be removed. Besides, it is a rational approach from practical viewpoint to assign pilots taken from different sets for CFUEs and DUEs.

Therefore, for a total of τ orthogonal pilots we consider $\tau_d = \max \left\{ \left\lfloor \frac{L}{L+K} \tau \right\rfloor, 1 \right\}$ of them for DUEs and the remaining $\tau_c = \tau - \tau_d$ for CFUEs, so that $\omega_k^H \theta_l = 0, \forall k, l$. Next, we resort to the greedy approach for assigning τ_c orthogonal pilots among K CFUEs [2]. The greedy-based CFUE pilot allocation (GCPA) is given in Algorithm 1. This algorithm starts with an initial random pilot allocation; then, the SE of the CFUEs are computed and the user with the minimum data rate is selected and allocated with a pilot that minimizes the pilot contamination term resulting from other CFUEs. Then, these steps are repeated for the newly assigned pilots for a limited number of iterations.

With respect to the DUEs, we use a modified version of graph coloring (GC) algorithm [28], [44] for allocating τ_d orthogonal pilots among L DUEs. By using GC-based pilot allocation the

Algorithm 2 Modified GC-based DUE pilot assignment

Input: Interference strengths $\varphi_{ll'}$, $\forall \{l, l'\}$, set of available orthogonal pilots $\Theta = \{\theta_1, \dots, \theta_{\tau_d}\}$, set of all the transmitters of D2D pairs \mathcal{L} , set of users that are assigned with pilots $\mathcal{U} = \emptyset$ which is empty initially, iteration index $\ell = 1$.

I. Iteration ℓ :

- I.1. Among all the D2D transmitters which are not assigned with pilot find the one that experiences or causes the largest interference

$$\hat{l} = \arg \max_{l' \in \mathcal{L} \setminus \mathcal{U}} \sum_{l \in \mathcal{L}} \varphi_{ll'}.$$

- I.2. From the set of available pilots, i.e. Θ , select the one that minimizes interference to the users with the same pilot sequence,

$$\theta_{\hat{l}} = \arg \min_{\pi_l \in \Theta} \sum_{l \in \mathcal{U}} \varphi_{l\hat{l}} \left| \theta_l^H \pi_{\hat{l}} \right|^2,$$

$$\mathcal{U} = \mathcal{U} \cup \hat{l}.$$

- II.** If $\ell = L$ stop. Otherwise $\ell = \ell + 1$ and go to **I**.

Output: The assigned pilots $\theta_l \forall l$.

potential interference due to reusing pilots between l th and l' th DUE transmitters at their desired receiver is denoted by $\varphi_{ll'}$ and is defined as

$$\varphi_{ll'} = \begin{cases} 0, & \text{if } l = l' \\ \frac{\psi_{ll'}^d}{\psi_{ll}^d} + \frac{\psi_{l'l}^d}{\psi_{l'l'}^d}, & \text{if } l \neq l' \end{cases} \quad (21)$$

So, a large $\varphi_{ll'}$ infers a strong interference at the receivers of l th and l' th D2D pairs by the other D2D pair's transmitter. The Modified GC-based DUE pilot assignment (MGCDPA) algorithm, which is given in Algorithm 2, attempts to allocate the pilots such that the users with the same pilot experience a low value of $\varphi_{ll'}$.

B. Power Allocation

We now consider transmit power allocation to further improve the system performance. We focus on the following two optimization problems:

- **Max Sum Rate of CFUEs subject to Quality of services for DUEs (MSRCQD),**
- **Weighted Max Product of SINRs of CFUEs and DUEs (WMPCD).**

In MSRCQD the sum data rate of the CFUEs are maximized while DUEs are constrained to have larger data rates than a predetermined value. In WMPCD, the objective is to maximize

the weighted product of SINRs of CFUEs and DUEs. This utility function tries to improve the overall performance of the system while providing a degree of fairness between the users, and thus all the users are served with a non-zero data rate [45].

- The MSRCQD optimization problem is formulated as follows

$$\mathcal{P}_1 : \begin{cases} \text{maximize} & \sum_{k=1}^K R_{k, \text{UatF}}^{\text{CFUEIP}} \\ \text{subject to} & R_{l, \text{apx}}^{\text{DUEIP}} \geq R_{l, \text{min}}, \quad l = 1, 2, \dots, L, \\ & \eta_k^c \leq 1, \quad k = 1, 2, \dots, K \\ & \eta_l^d \leq 1, \quad l = 1, 2, \dots, L. \end{cases} \quad (22)$$

\mathcal{P}_1 is a non-convex and NP-hard problem to solve optimally.

Theorem 5. *Solution of problem \mathcal{P}_1 can approximately be efficiently obtained using the following GP problem.*

$$\mathcal{P}'_1 : \begin{cases} \text{maximize} & \prod_{k=1}^K v_k \\ \text{subject to} & \frac{v_k B_k(\eta^c, \eta^d)}{A_k(\eta_k^c)} \leq 1, \\ & \frac{\zeta_l D_l(\eta^c, \eta^d)}{C_l(\eta_k^c)} \leq 1, \\ & \eta_k^c \leq 1, \quad \eta_l^d \leq 1, \\ & k = 1, 2, \dots, K, \quad l = 1, 2, \dots, L. \end{cases} \quad (23)$$

Where $A_k(\eta_k^c)$ and $C_l(\eta_l^d)$ are the numerator of the SINR of the k th CFUE and the l th DUE reported in (17) and (20), respectively. Also, $B_k(\eta^c, \eta^d)$ and $D_l(\eta^c, \eta^d)$ are the corresponding denominators, and $\eta^c = \{\eta_1^c, \dots, \eta_K^c\}$, $\eta^d = \{\eta_1^d, \dots, \eta_L^d\}$, $\zeta_l = 2^{R_{l, \text{min}}/\varsigma} - 1$.

Proof. By assuming high SINR approximation for CFUEs, the objective function in \mathcal{P}_1 after ignoring "1" in rate expression inside the logarithm in (17) becomes $\sum_{k=1}^K R_{k, \text{UatF}}^{\text{CFUEIP}} \approx \varsigma \sum_{k=1}^K \log \left(\frac{A_k(\eta_k^c)}{B_k(\eta^c, \eta^d)} \right) = \varsigma \log \left(\prod_{k=1}^K \frac{A_k(\eta_k^c)}{B_k(\eta^c, \eta^d)} \right)$. Then by removing the constant coefficient ς and ignoring the monotonically increasing function, i.e. the logarithm, the optimizing values

of optimization variables will remain unchanged.

Next, we introduce the auxiliary variable v_k such that $\frac{A_k(\eta_k^c)}{B_k(\eta^c, \eta^d)} \geq v_k$ which results the first constraint and the objective of \mathcal{P}'_1 . Since $A_k(\eta_k^c)$, $C_l(\eta_l^d)$, and the objective in \mathcal{P}'_1 are monomial and $B_k(\eta^c, \eta^d)$, $D_l(\eta^c, \eta^d)$ are posynomial, the inequality constraints are posynomial, and thus problem (23) is a GP problem. \square

- The second problem that we investigate is WMPCD which is formulated as \mathcal{P}_2

$$\mathcal{P}_2 : \begin{cases} \text{maximize} & \left(\prod_{k=1}^K \frac{A_k(\eta_k^c)}{B_k(\eta^c, \eta^d)} \right)^{w^c} \left(\prod_{l=1}^L \frac{C_l(\eta_l^d)}{D_l(\eta^c, \eta^d)} \right)^{w^d} \\ \text{subject to} & \eta_k^c \leq 1, \quad k = 1, 2, \dots, K, \\ & \eta_l^d \leq 1, \quad l = 1, 2, \dots, L. \end{cases} \quad (24)$$

It is worth mentioning that the first and the second terms in the objective function of \mathcal{P}_2 are the product of the SINRs of CFUEs and DUEs respectively, and $w^c \geq 0$, $w^d \geq 0$ are the respective weights. Solution of the above optimization problem is addressed in the following theorem.

Theorem 6. *Solution of the optimization problem \mathcal{P}_2 can be obtained from following GP problem.*

$$\mathcal{P}'_2 : \begin{cases} \text{maximize} & \left(\prod_{k=1}^K v_k \right)^{w^c} \left(\prod_{l=1}^L x_l \right)^{w^d} \\ \text{subject to} & \frac{v_k B_k(\eta^c, \eta^d)}{A_k(\eta_k^c)} \leq 1, \\ & \frac{x_l D_l(\eta^c, \eta^d)}{C_l(\eta_l^d)} \leq 1, \\ & \eta_k^c \leq 1, \quad \eta_l^d \leq 1, \\ & k = 1, 2, \dots, K, \quad l = 1, 2, \dots, L. \end{cases} \quad (25)$$

Proof. For obtaining \mathcal{P}'_2 we first introduce the auxiliary variables v_k and x_l such that $\frac{A_k(\eta_k^c)}{B_k(\eta^c, \eta^d)} \geq v_k$ and $\frac{C_l(\eta_l^d)}{D_l(\eta^c, \eta^d)} \geq x_l$, $\forall l, k$. Then, after rearranging these inequalities, the two first constraints are derived. Similar to the proof of theorem 5, the inequality constraints are

posynomial while the objective function is monomial therefore \mathcal{P}'_2 is a GP problem. \square

In the subsequent section numerical results are provided to evaluate the system performance of the proposed pilot and power allocation problems.

V. NUMERICAL RESULTS

We focus on a simulation scenario with $K = 20$ CFUEs, $L = 10$ pairs of D2D users, $M = 200$ APs, and $b = 4$ bits, unless specifically mentioned, which are uniformly and randomly distributed within area of $D = 1 \times 1$ [km²]. Moreover, for each pair of D2D users we assume that the transmitter and the receiver are randomly placed within a distance of 10 [m] up to 100 [m] from one another. In addition, we use wrapping technique to avoid boundary effect. The large-scale fading follows a three-slope model as below [18].

$$\beta_{mk} = PL_{mk} + \sigma_{sh} z_{mk}$$

$$PL_{mk} = \begin{cases} -L - 10 \log_{10}(d_{mk}^{3.5}), & \text{if } d_{mk} \geq d_1 \\ -L - 10 \log_{10}(d_1^{1.5} d_{mk}^2), & \text{if } d_0 < d_{mk} \leq d_1 \\ -L - 10 \log_{10}(d_1^{1.5} d_0^2), & \text{if } d_{mk} \leq d_0 \end{cases}$$

$$L = 46.3 + 33.9 \log_{10}(f) - 13.82 \log_{10}(h_{AP}) - (1.1 \log_{10}(f) - 0.7)h_u + (1.56 \log_{10}(f) - 0.8), \quad (26)$$

where, $\sigma_{sh} = 8$ [dB], $z_{mk} \sim \mathcal{CN}(0, 1)$ are shadowing parameters, and PL_{mk} is path-loss in [dB]. Also, $h_{AP} = 15$ [m], $h_u = 1.65$ [m], $f = 1900$ [MHz] are the APs height, user antenna height and carrier frequency, respectively, additionally, $d_0 = 10$ [m], $d_1 = 50$ [m]. The noise power is computed by $N = B \times k_B \times T_0 \times NF$ where, $B = 20$ [MHz], $k_B = 1.381 \times 10^{-23}$ [Joule/Kelvin], $T_0 = 290$ [Kelvin] and $NF = 9$ [dB] are system bandwidth, Boltzmann constant, temperature and noise figure, respectively. Also, $T = 200$ samples, $\rho^c = \rho^d = 100$ [mW], $\rho_p^c = \rho_p^d = 200$ [mW], and $\tau = 10$ are considered.

Fig. 2a and Fig. 2b address the impact of the number of D2D pairs, i.e. L , on the data rate of CFUEs and DUEs. From Fig. 2a, it is seen that by adding more D2D pairs to the system, the average data rates of both CFUEs and DUEs are decreased. This reduction in per user data rate

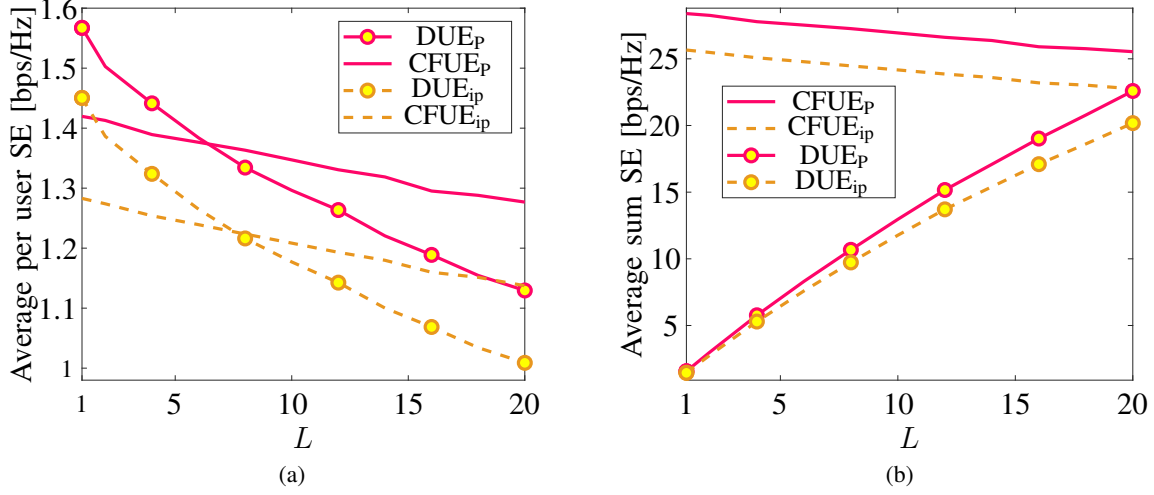


Fig. 2. The impact of the number of DUEs on the data rate of CFUEs and DUEs with full power allocation. (a) Per user data rate. (b) Sum data rate.

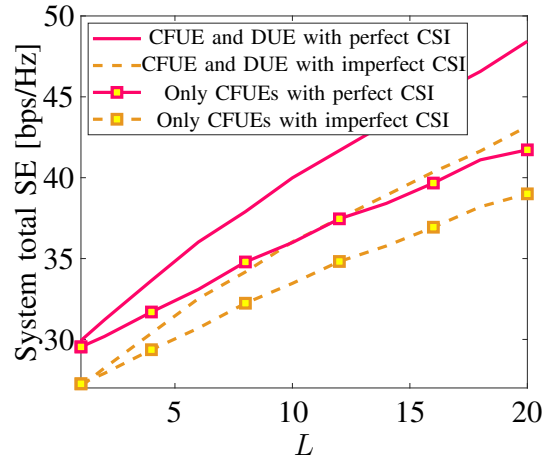


Fig. 3. The advantages of considering D2D users in a CF-mMIMO system.

comes from the increase in interference caused by the new DUEs. Therefore, the sum data rate of CFUEs are also decreased; however, the sum data rate of DUEs are increased due to increase in the number of DUEs.

Now we compare performance of two systems; one serves simultaneously L DUEs and K CFUEs, and the other one *only* supports $K + L$ CFUEs without serving D2D users. In Fig. 3, the system total SE, i.e. sum of DUEs and CFUEs SEs, versus L is depicted for perfect and imperfect CSI with full power allocation. It is shown that to improve the system total SE, it is

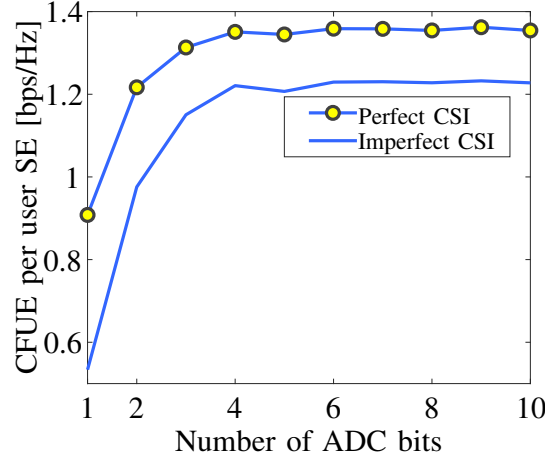


Fig. 4. The effect of the number of ADC bits, i.e. b , on the data rate with perfect and imperfect CSI and full power allocation.

reasonable to simultaneously support CFUEs and DUEs. That is, for users with the possibility of establishing D2D communications, it is better to communicate through D2D links instead of using mobile infrastructure.

Figure 4 depicts the achievable data rate of CFUEs when ADCs with different number of bits are deployed at the APs. By increasing the number of ADCs' bits the quantization noise is decreased and the performance improves. For ADCs with more than 4 bits the improvements are marginal, so we set $b = 4$ in the remainder of this section.

The performance of the system with MSRCQD power control and different QoSs for DUEs are investigated in Fig. 5. Fig. 5a represents the result for per user data rate of CFUEs, as one can see from this figure when the QoS for DUEs are set to be 0.5 [bps/Hz], there is 10% improvement in the data rate of CFUEs. For, smaller R_{\min} , this improvement is even larger; because, lower power is assigned to the DUEs and the interference is reduced. Similar discussions are true in case of Fig. 5b and Fig. 5c.

Fig. 6 addresses the CDF of per user and sum rate of CFUEs, and the minimum data rate of DUEs in Fig. 6a, Fig. 6b and Fig. 6c. By checking the 5%-outage rate, it can be found that the MSRCQD power allocation along with the pilot assignment can have near 38% and 16% improvements compared to full power and random pilot assignment. Also, DUEs satisfy the QoS constraint as shown in Fig. 6c.

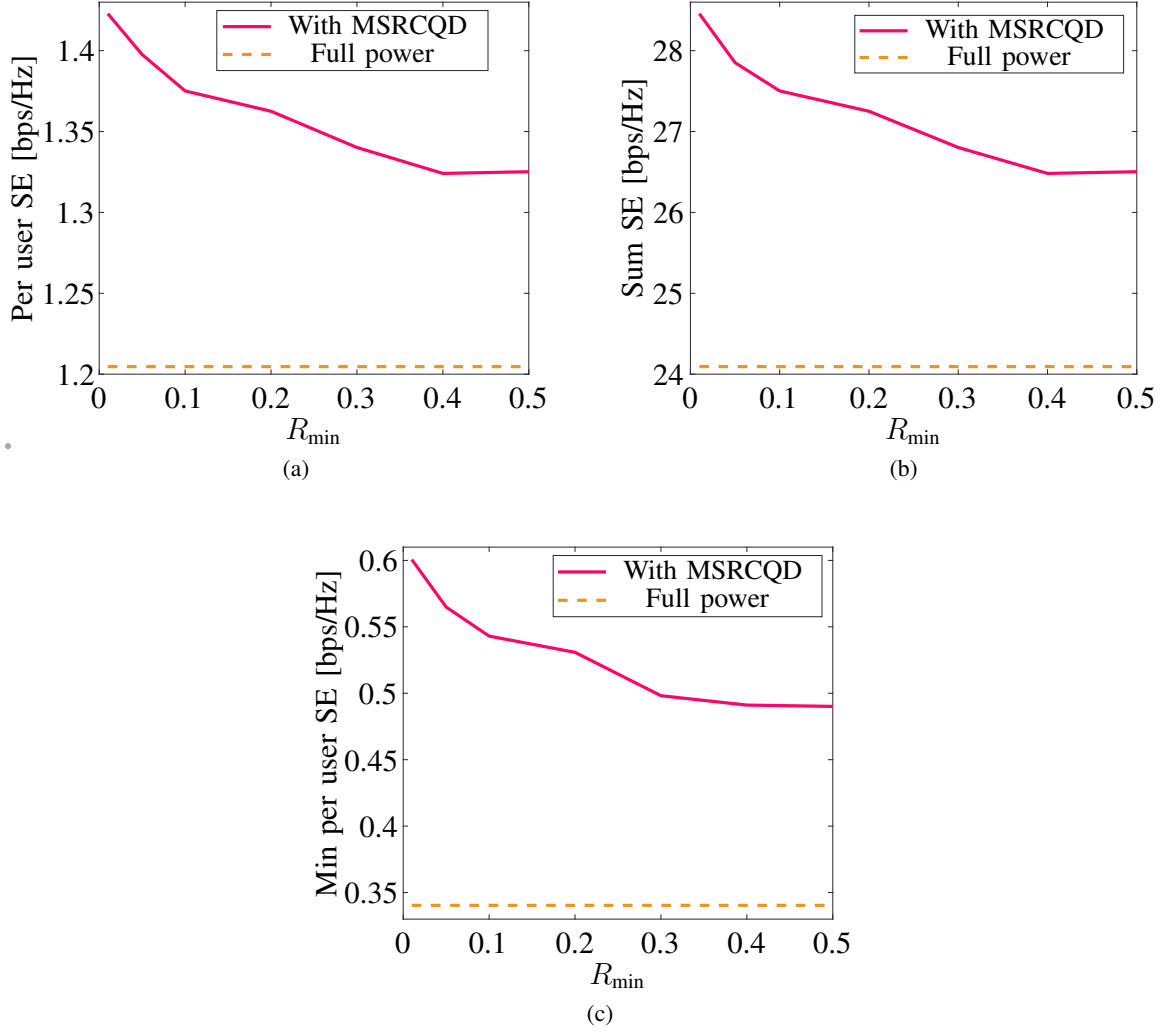


Fig. 5. Performance of CFUEs without pilot allocation and power control and with pilot allocation and MSRCQD power control for different QoSs for DUEs, i.e. R_{\min} . (a) Per user SE. (b) Sum SE. (c) minimum SE.

In Fig. 7, performance of the system with the WMPCD power control for different weights is evaluated. Note that, R_{\min}^{opt} , R^{opt} and R_{sum}^{opt} are indicating minimum rate among the users, per user rate and sum rate of the users with WMPCD power control and pilot assignment, respectively, while those without the superscript opt are the corresponding rates for full power and random pilot assignment. Therefore, when the curves are above the horizontal dot-line, we have performance improvements compared to that of without resource allocation. For smaller w^c , it means higher priority to DUEs, so the objective function is maximized by improving the DUEs data rate and cutting down the interference from CFUEs. As a result, less power is

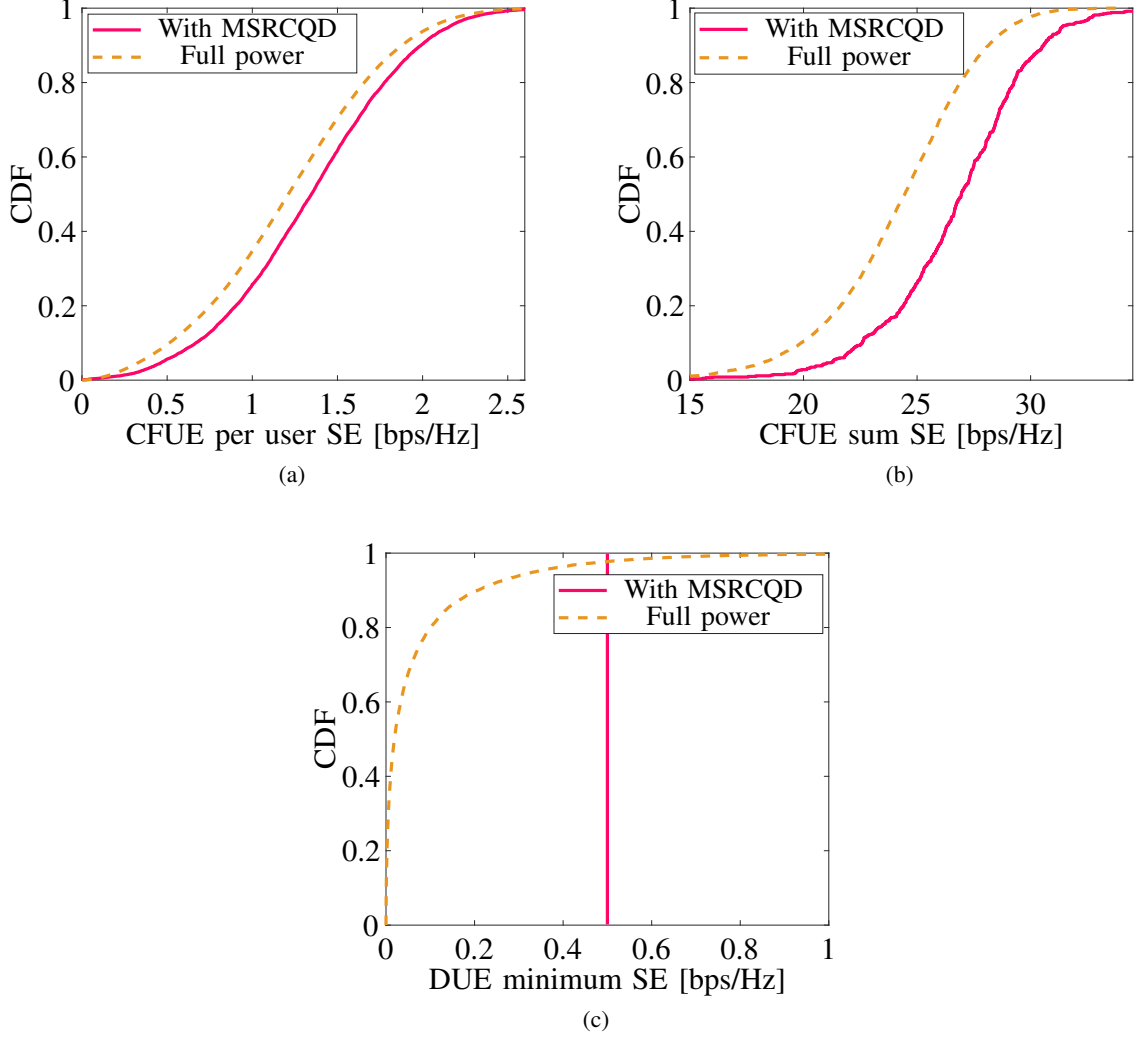


Fig. 6. CDF without pilot and power allocation and with pilot allocation and MSRCQD power control and $R_{\min} = 0.5$ [bps/Hz] for all DUEs. (a) CFUE per user SE. (b) CFUE sum SE. (c) DUE minimum SE.

dedicated for data transmission of CFUEs. On the other hand, when w^c gets closer to 1, similarly the behaviour of the system is justifiable. Moreover, the performance improvement is much more pronounced for the minimum rate, as depicted in Fig. 7a, which shows near 50% improvement for both DUEs and CFUEs (for the case $w^c \approx 0.5$). Regarding instead the per user rate and sum data rate, the same performance enhancement for both types of users occurs around $w^c \approx 0.6$. Also, as it is observed from these figures for $0.3 \leq w^c \leq 0.8$ we have improvements for both DUEs and CFUEs, though by varying w^c in the given interval one can reach different trade-offs between CFUEs and DUEs.

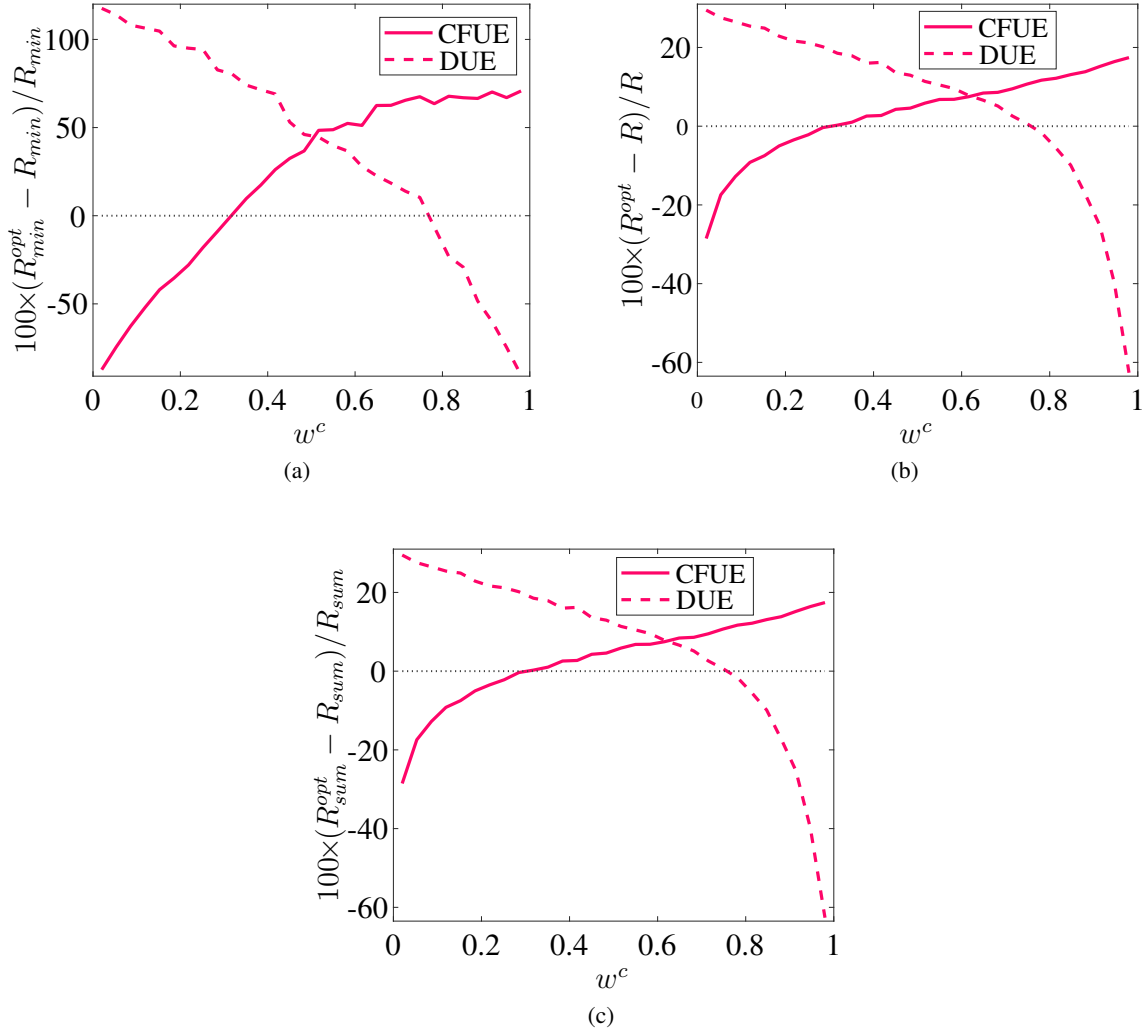


Fig. 7. Performance of DUEs and CFUEs, without pilot allocation and power control and with pilot allocation and WMPCD power control for different values of weight $w^c = 1 - w^d$ where $w^c \in [0, 1]$. (a) minimum SE. (b) Per user SE. (c) Sum SE.

VI. CONCLUSIONS

We studied a D2D underlaid CF-mMIMO system in the uplink mode wherein APs were equipped with low resolution ADCs. For the cases of both perfect and imperfect CSI at the receivers, closed-form expressions of achievable data rates for both CFUEs and DUEs were derived. In order to obtain estimates of D2D pairs' and CFUEs' channels, we considered a set of orthogonal pilot sequences that were reused among DUEs and CFUEs. We also adopted greedy-based and graph coloring-based algorithms to assign pilot sequences among different users, in order to control the resultant pilot contamination. Next, two power allocation problems

were explored: the former maximizes the CFUEs' sum SE subject to QoS constraints on DUEs data rates; the latter maximizes the weighted product of SINRs of CFUEs and DUEs. In both problems, users were also subject to a maximum transmit power constraint and GP theory was used to solve both problems. Then, we provided numerical results wherein we studied the impact of the number of DUEs, and of the resolution of the ADCs. Results have shown that using 4-bit ADCs at the APs can provide almost the same performance as that of the infinite resolution ADCs'. Additionally, activating D2D links improves the overall SE with respect to the case in which all the communications flow through the network infrastructure. Finally, a significant performance enhancement for the system with the presented pilot assignment algorithms and power allocation procedures has been observed in comparison with the benchmark case of random pilot allocation and full power transmission.

APPENDIX A

It can be shown that all the terms in \mathcal{I}_k^c are mutually uncorrelated, therefore

$$\begin{aligned}\mathbb{E}\{\mathbf{DS}_k\} &= \xi \sqrt{\eta_k^c \rho^c} \sum_{m=1}^M \mathbb{E}\{|h_{mk}^c|^2\} = \xi \sqrt{\eta_k^c \rho^c} \sum_{m=1}^M \beta_{mk}^c, \\ \mathbb{E}\{\mathbf{BU}_k\} &= \xi^2 \eta_k^c \rho^c \mathbb{E}\left\{\left|\sum_{m=1}^M |h_{mk}^c|^2 - \sum_{m=1}^M \mathbb{E}\{|h_{mk}^c|^2\}\right|^2\right\} = \xi^2 \eta_k^c \rho^c \mathbb{E}\left\{\left|\sum_{m=1}^M (|h_{mk}^c|^2 - \beta_{mk}^c)\right|^2\right\}.\end{aligned}\quad (27)$$

Since the terms $(|h_{mk}^c|^2 - \beta_{mk}^c)$ are uncorrelated for different m , the above equation (27) can be simplified as

$$\mathbb{E}\{\mathbf{BU}_k\} = \xi^2 \eta_k^c \rho^c \sum_{m=1}^M \mathbb{E}\{|h_{mk}^c|^2 - \beta_{mk}^c\} = \xi^2 \eta_k^c \rho^c \sum_{m=1}^M (\mathbb{E}\{|h_{mk}^c|^4\} - \beta_{mk}^{c^2}) \stackrel{(a)}{=} \xi^2 \eta_k^c \rho^c \sum_{m=1}^M \beta_{mk}^{c^2}, \quad (28)$$

where (a) is due to $\mathbb{E}\{|h_{mk}^c|^4\} = 2\beta_{mk}^{c^2}$. Also, for computing $\text{Var}(\mathcal{I}_k^c)$ we have

$$\text{Var}(\mathcal{I}_k^c) = \mathbb{E}\{|\mathcal{I}_k^c|^2\} - \underbrace{|\mathbb{E}\{\mathcal{I}_k^c\}|^2}_{=0} = \mathbb{E}\{|\mathbf{ICFUE}_k|^2\} + \mathbb{E}\{|\mathbf{IDUE}_k|^2\} + \mathbb{E}\{|\mathbf{TN}_k|^2\} + \mathbb{E}\{|\mathbf{QN}_k|^2\}. \quad (29)$$

By computing each of the terms in the above equation, we have

$$\begin{aligned}\mathbb{E}\{| \text{ICFUE}_k |^2\} &= \xi^2 \rho^c \sum_{k' \neq k}^K \eta_{k'}^c \mathbb{E} \left\{ \left| \sum_{m=1}^M h_{mk}^{c*} h_{mk'}^c \right|^2 \right\} = \xi^2 \rho^c \sum_{k' \neq k}^K \eta_{k'}^c \sum_{m=1}^M \mathbb{E} \{ |h_{mk}^{c*} h_{mk'}^c|^2 \} \\ &= \xi^2 \rho^c \sum_{k' \neq k}^K \eta_{k'}^c \sum_{m=1}^M \beta_{mk}^c \beta_{mk'}^c,\end{aligned}\quad (30)$$

$$\begin{aligned}\mathbb{E}\{| \text{IDUE}_k |^2\} &= \xi^2 \rho^d \sum_{l'=1}^L \eta_{l'}^d \mathbb{E} \left\{ \left| \sum_{m=1}^M h_{mk}^{c*} h_{ml'}^d \right|^2 \right\} = \xi^2 \rho^d \sum_{l'=1}^L \eta_{l'}^d \sum_{m=1}^M \mathbb{E} \{ |h_{mk}^{c*} h_{ml'}^d|^2 \} \\ &= \xi^2 \rho^d \sum_{l'=1}^L \eta_{l'}^d \sum_{m=1}^M \beta_{mk}^c \beta_{ml'}^d,\end{aligned}\quad (31)$$

$$\mathbb{E}\{| \text{TN}_k |^2\} = \xi^2 \mathbb{E} \left\{ \left| \sum_{m=1}^M h_{mk}^{c*} n_m \right|^2 \right\} = \xi^2 \sum_{m=1}^M \mathbb{E} \{ |h_{mk}^{c*} n_m|^2 \} = \xi^2 N_0 \sum_{m=1}^M \beta_{mk}^c, \quad (32)$$

$$\begin{aligned}\mathbb{E}\{| \text{QN}_k |^2\} &= \mathbb{E} \left\{ \left| \sum_{m=1}^M h_{mk}^{c*} q_m \right|^2 \right\} = \sum_{m=1}^M \mathbb{E} \{ |h_{mk}^c|^2 \mathbb{E} \{ |q_m|^2 | \{h_{mt}\} \} \} \stackrel{(3)}{=} \sum_{m=1}^M \mathbb{E} \{ |h_{mk}^c|^2 (1-\xi) \xi \\ &\times \left(\rho^c \sum_{k'=1}^K \eta_{k'}^c |h_{mk'}^c|^2 + \rho^d \sum_{l'=1}^L \eta_{l'}^d |h_{ml'}^d|^2 + N_0 \right) \} = (1-\xi) \xi \left(\rho^c \sum_{m=1}^M \sum_{k'=1}^K \eta_{k'}^c \mathbb{E} \{ |h_{mk}^c|^2 |h_{mk'}^c|^2 \} \right. \\ &+ \rho^d \sum_{m=1}^M \sum_{l'=1}^L \eta_{l'}^d \mathbb{E} \{ |h_{mk}^c|^2 |h_{ml'}^d|^2 \} + N_0 \sum_{m=1}^M \beta_{mk}^c \Big) = (1-\xi) \xi \rho^c \sum_{k'=1}^K \eta_{k'}^c \sum_{m=1}^M \beta_{mk}^c \beta_{mk'}^c \\ &+ (1-\xi) \xi \rho^c \sum_{m=1}^M \beta_{mk}^{c^2} + (1-\xi) \xi \rho^d \sum_{l'=1}^L \eta_{l'}^d \sum_{m=1}^M \beta_{mk}^c \beta_{ml'}^d + (1-\xi) \xi N_0 \sum_{m=1}^M \beta_{mk}^c,\end{aligned}\quad (33)$$

By combining equations (27)–(33) and using (8) the achievable rate is derived.

APPENDIX B

According to (12) we approximate R_l^{DUEp} with $R_{l,\text{apx}}^{\text{DUEp}}$ which is given by

$$R_{l,\text{apx}}^{\text{DUEp}} = \log_2 \left(1 + \left(\mathbb{E} \left\{ \frac{\rho^c \sum_{k=1}^K \eta_k^c |\bar{g}_{lk}^{d,c}|^2 + \rho^d \sum_{l' \neq l}^L \eta_{l'}^d |\bar{g}_{ll'}^d|^2 + N_0}{\rho^d \eta_l^d \|\mathbf{g}_{ll}^d\|^2} \right\} \right)^{-1} \right), \quad (34)$$

where $\bar{g}_{lk}^{d,c} = \frac{\mathbf{g}_{ll}^{dH} \mathbf{g}_{lk}^c}{\|\mathbf{g}_{ll}^d\|}$ and $\bar{g}_{ll'}^d = \frac{\mathbf{g}_{ll}^{dH} \mathbf{g}_{ll'}^c}{\|\mathbf{g}_{ll}^d\|}$ which are $\mathcal{CN}(0, \psi_{lk}^c)$ and $\mathcal{CN}(0, \psi_{ll'}^d)$ conditioned on \mathbf{g}_{ll}^d respectively [46], so we can write

$$\begin{aligned} \mathbb{E} \left\{ \frac{\rho^c \sum_{k=1}^K \eta_k^c |\bar{g}_{lk}^{d,c}|^2 + \rho^d \sum_{l' \neq l}^L \eta_{l'}^d |\bar{g}_{ll'}^d|^2 + N_0}{\rho^d \eta_l^d \|\mathbf{g}_{ll}^d\|^2} \right\} &= \mathbb{E} \left\{ \rho^c \sum_{k=1}^K \eta_k^c |\bar{g}_{lk}^{d,c}|^2 + \rho^d \sum_{l' \neq l}^L \eta_{l'}^d |\bar{g}_{ll'}^d|^2 + N_0 \right\} \\ &\times \mathbb{E} \left\{ \frac{1}{\rho^d \eta_l^d \|\mathbf{g}_{ll}^d\|^2} \right\} \stackrel{(a)}{=} \frac{\rho^c \sum_{k=1}^K \eta_k^c \psi_{lk}^c + \rho^d \sum_{l' \neq l}^L \eta_{l'}^d \psi_{ll'}^d + N_0}{\rho^d \eta_l^d \psi_{ll}^d (N-1)}, \end{aligned} \quad (35)$$

where (a) comes from the fact that \mathbf{g}_{ll}^d can be written as $\mathbf{g}_{ll}^d = \sqrt{\psi_{ll}^d} \mathbf{w}$ such that $\mathbf{w} \sim \mathcal{CN}(0, \mathbf{I}_N)$, also $\|\mathbf{w}\|^2 = \frac{1}{2} \sum_{n=1}^{2N} x_n^2$ and $x_n \sim \mathcal{N}(0, 1)$, $\forall n$. Therefore, $\frac{1}{\|\mathbf{g}_{ll}^d\|^2} = \frac{1}{\psi_{ll}^d \|\mathbf{w}\|^2} = \frac{2}{\psi_{ll}^d \sum_{n=1}^{2N} x_n^2}$ where $\frac{1}{\sum_{n=1}^{2N} x_n^2}$ has inverse Chi-squared distribution with $2N$ degrees of freedom with $\mathbb{E} \left\{ \frac{1}{\sum_{n=1}^{2N} x_n^2} \right\} = \frac{1}{2N-2}$ which results in

$$\begin{aligned} \mathbb{E} \left\{ \frac{1}{\rho^d \eta_l^d \|\mathbf{g}_{ll}^d\|^2} \right\} &= \mathbb{E} \left\{ \frac{2}{\rho^d \eta_l^d \psi_{ll}^d \sum_{n=1}^{2N} x_n^2} \right\} = \frac{2}{\rho^d \eta_l^d \psi_{ll}^d} \mathbb{E} \left\{ \frac{1}{\sum_{n=1}^{2N} x_n^2} \right\} \\ &= \frac{2}{\rho^d \eta_l^d \psi_{ll}^d} \times \frac{1}{2(N-1)} = \frac{1}{\rho^d \eta_l^d \psi_{ll}^d (N-1)}. \end{aligned} \quad (36)$$

APPENDIX C

By performing MRC and UatF for the k th CFUE, the following estimation of its symbol is detected at the CPU

$$\begin{aligned} r_k^c &= \sum_{m=1}^M \hat{h}_{mk}^{c*} y_m^c = \underbrace{\xi \sqrt{\eta_k^c \rho^c} \mathbb{E} \left\{ \sum_{m=1}^M \hat{h}_{mk}^{c*} h_{mk}^c \right\}}_{\text{DS}_k: \text{desired signal}} s_k^c + \underbrace{\xi \sqrt{\eta_k^c \rho^c} \left\{ \sum_{m=1}^M \hat{h}_{mk}^{c*} h_{mk}^c - \mathbb{E} \left\{ \sum_{m=1}^M \hat{h}_{mk}^{c*} h_{mk}^c \right\} \right\}}_{\text{BU}_k: \text{Beamforming Uncertainty}} s_k \\ &+ \underbrace{\xi \sqrt{\rho^c} \sum_{k' \neq k}^K \sqrt{\eta_{k'}^c} \sum_{m=1}^M \hat{h}_{mk}^{c*} h_{mk'}^c s_{k'}^c}_{\text{ICFUE}_k: \text{interference from CFUEs}} + \underbrace{\xi \sqrt{\rho^d} \sum_{l'=1}^L \sqrt{\eta_{l'}^d} \sum_{m=1}^M \hat{h}_{mk}^{c*} h_{ml'}^d s_{l'}^d}_{\text{IDUE}_k: \text{interference from DUEs}} + \underbrace{\xi \sum_{m=1}^M \hat{h}_{mk}^{c*} n_m}_{\text{TN}_k: \text{total noise}} + \underbrace{\sum_{m=1}^M \hat{h}_{mk}^{c*} q_m}_{\text{QN}_k: \text{quantization noise}}, \end{aligned} \quad (37)$$

where, \hat{h}_{mk}^c is given in (15) and the interfering terms are collectively denoted by $\mathcal{I}_k^c = \text{BU}_k + \text{ICFUE}_k + \text{IDUE}_k + \text{TN}_k + \text{QN}_k$. It is worth mentioning that these terms are zero mean and mutually uncorrelated with one another and with the desired signal. Therefore by assuming that

the equivalent interference term \mathcal{I}_k^c follows the worst case scenario of Gaussian distribution, the achievable rate is expressed similar to (8). Also, $\text{Var}(\mathcal{I}_k^c) = \mathbb{E}\{|\mathcal{I}_k^c|^2\} - \underbrace{\mathbb{E}\{\mathcal{I}_k^c\}^2}_{=0} = \mathbb{E}\{|\text{BU}_k|^2\} + \mathbb{E}\{|\text{ICFUE}_k|^2\} + \mathbb{E}\{|\text{IDUE}_k|^2\} + \mathbb{E}\{|\text{TN}_k|^2\} + \mathbb{E}\{|\text{QN}_k|^2\}$. These terms are calculated in the following

$$\begin{aligned} \mathbb{E}\{\text{DS}_k\} &= \xi \sqrt{\eta_k^c \rho^c} \sum_{m=1}^M \mathbb{E}\{\hat{h}_{mk}^{c*} h_{mk}^c\} = \xi \sqrt{\eta_k^c \rho^c} \sum_{m=1}^M \gamma_{mk}^c, \\ \mathbb{E}\{\text{BU}_k\} &\stackrel{(a)}{=} \xi^2 \eta_k^c \rho^c \sum_{m=1}^M \mathbb{E}\left\{\left|\hat{h}_{mk}^{c*} h_{mk}^c - \gamma_{mk}^c\right|^2\right\} = \xi^2 \eta_k^c \rho^c \sum_{m=1}^M \gamma_{mk}^c \beta_{mk}^c + \xi(1-\xi) \eta_k^c \rho^c \sum_{m=1}^M \gamma_{mk}^c, \end{aligned} \quad (38)$$

where (a) is due to the fact that $(\hat{h}_{mk}^{c*} h_{mk}^c - \gamma_{mk}^c)$ is uncorrelated for different m .

$$\begin{aligned} \mathbb{E}\{|\text{ICFUE}_k|^2\} &= \xi^2 \rho^c \sum_{k' \neq k}^K \eta_{k'}^c \sum_{m=1}^M \mathbb{E}\left\{\left|\hat{h}_{mk}^{c*} h_{mk'}^c\right|^2\right\} = \xi^2 \rho^c \sum_{k' \neq k}^K \eta_{k'}^c \sum_{m=1}^M \gamma_{mk'}^c \beta_{mk'}^c \\ &\quad + \xi \rho^c \sum_{k' \neq k}^K \eta_{k'}^c \sum_{m=1}^M \left(\gamma_{mk}^c \frac{\sqrt{\mu_{k'}^c} \beta_{mk'}^c}{\sqrt{\mu_{k'}^c} \beta_{mk}^c}\right)^2 |\boldsymbol{\omega}_k^H \boldsymbol{\omega}_{k'}|^2, \end{aligned} \quad (39)$$

$$\begin{aligned} \mathbb{E}\{|\text{IDUE}_k|^2\} &= \xi^2 \rho^d \sum_{l'=1}^L \eta_{l'}^d \sum_{m=1}^M \mathbb{E}\left\{\left|\hat{h}_{mk}^{c*} h_{ml'}^d\right|^2\right\} = \xi^2 \rho^d \sum_{l'=1}^L \eta_{l'}^d \sum_{m=1}^M \gamma_{mk}^c \beta_{ml'}^d \\ &\quad + \xi \rho^d \sum_{l'=1}^L \eta_{l'}^d \sum_{m=1}^M \left(\gamma_{mk}^c \frac{\sqrt{\mu_{l'}^d} \rho_p^d \beta_{ml'}^d}{\sqrt{\mu_k^c} \rho_p^c \beta_{mk}^c}\right)^2 |\boldsymbol{\omega}_k^H \boldsymbol{\theta}_{l'}|^2, \end{aligned} \quad (40)$$

$$\mathbb{E}\{|\text{TN}_k|^2\} = \xi^2 \sum_{m=1}^M \mathbb{E}\left\{\left|\hat{h}_{mk}^{c*} n_m\right|^2\right\} = \xi^2 N_0 \sum_{m=1}^M \gamma_{mk}^c, \quad (41)$$

$$\begin{aligned} \mathbb{E}\{|\text{QN}_k|^2\} &= \sum_{m=1}^M \mathbb{E}\left\{\mathbb{E}\left\{\left|\hat{h}_{mk}^{c*} q_m\right|^2 \middle| \{h_{mt_i}\}\right\}\right\} = \xi(1-\xi) \rho^c \sum_{k'=1}^K \eta_{k'}^c \sum_{m=1}^M \gamma_{mk}^c \beta_{mk'}^c \\ &\quad + \xi(1-\xi) \rho^d \sum_{l'=1}^L \eta_{l'}^d \sum_{m=1}^M \gamma_{mk}^c \beta_{ml'}^d + (1-\xi) \rho^c \sum_{k'=1}^K \eta_{k'}^c \sum_{m=1}^M \left(\gamma_{mk}^c \frac{\sqrt{\mu_{k'}^c} \beta_{mk'}^c}{\sqrt{\mu_{k'}^c} \beta_{mk}^c}\right)^2 |\boldsymbol{\omega}_k^H \boldsymbol{\omega}_{k'}|^2 \\ &\quad + (1-\xi) \rho^d \sum_{l'=1}^L \eta_{l'}^d \sum_{m=1}^M \left(\gamma_{mk}^c \frac{\sqrt{\mu_{l'}^d} \rho_p^d \beta_{ml'}^d}{\sqrt{\mu_k^c} \rho_p^c \beta_{mk}^c}\right)^2 |\boldsymbol{\omega}_k^H \boldsymbol{\theta}_{l'}|^2 + \xi(1-\xi) N_0 \gamma_{mk}, \end{aligned} \quad (42)$$

By combining equations (38)–(42) the thesis of Theorem 3 is obtained.

REFERENCES

- [1] N. Rajatheva, I. Atzeni, E. Bjornson, A. Bourdoux, S. Buzzi, J.-B. Dore, S. Erkucuk, M. Fuentes, K. Guan, Y. Hu, *et al.*, “White paper on broadband connectivity in 6G,” *arXiv preprint arXiv:2004.14247*, 2020.
- [2] H. Q. Ngo, A. Ashikhmin, H. Yang, E. G. Larsson, and T. L. Marzetta, “Cell-free massive MIMO versus small cells,” *IEEE Transactions on Wireless Communications*, vol. 16, no. 3, pp. 1834–1850, 2017.
- [3] E. Nayebe, A. Ashikhmin, T. L. Marzetta, H. Yang, and B. D. Rao, “Precoding and power optimization in cell-free massive MIMO systems,” *IEEE Transactions on Wireless Communications*, vol. 16, no. 7, pp. 4445–4459, 2017.
- [4] S. Zhang, J. Liu, H. Guo, M. Qi, and N. Kato, “Envisioning device-to-device communications in 6G,” *Early Access in IEEE network*, 2020.
- [5] L. Song, D. Niyato, Z. Han, and E. Hossain, *Wireless device-to-device communications and networks*. Cambridge University Press, 2015.
- [6] K. M. S. Huq, S. Mumtaz, J. Rodriguez, P. Marques, B. Okyere, and V. Frasca, “Enhanced C-RAN using D2D network,” *IEEE Communications Magazine*, vol. 55, no. 3, pp. 100–107, 2017.
- [7] S. Buzzi, C. DAndrea, A. Zappone, and C. DElia, “User-centric 5G cellular networks: Resource allocation and comparison with the cell-free massive MIMO approach,” *IEEE Transactions on Wireless Communications*, vol. 19, no. 2, pp. 1250 – 1264, 2019.
- [8] E. Björnson and L. Sanguinetti, “Making cell-free massive MIMO competitive with MMSE processing and centralized implementation,” *IEEE Transactions on Wireless Communications*, vol. 19, no. 1, pp. 77–90, 2019.
- [9] H. Q. Ngo, L.-N. Tran, T. Q. Duong, M. Matthaiou, and E. G. Larsson, “On the total energy efficiency of cell-free massive MIMO,” *IEEE Transactions on Green Communications and Networking*, vol. 2, no. 1, pp. 25–39, 2018.
- [10] T. Van Chien, E. Björnson, and E. G. Larsson, “Joint power allocation and load balancing optimization for energy-efficient cell-free massive MIMO networks,” *arXiv preprint arXiv:2002.01504*, 2020.
- [11] T. C. Mai, H. Q. Ngo, M. Egan, and T. Q. Duong, “Pilot power control for cell-free massive MIMO,” *IEEE Transactions on Vehicular Technology*, vol. 67, no. 11, pp. 11264–11268, 2018.
- [12] S. Buzzi, C. D’Andrea, M. Fresia, Y.-P. Zhang, and S. Feng, “Pilot assignment in cell-free massive MIMO based on the Hungarian algorithm,” *arXiv preprint arXiv:2004.06940*, 2020.
- [13] P. Liu, K. Luo, D. Chen, and T. Jiang, “Spectral efficiency analysis of cell-free massive MIMO systems with zero-forcing detector,” *IEEE Transactions on Wireless Communications*, vol. 19, no. 2, pp. 795–807, 2019.
- [14] G. Femenias, N. Lassoued, and F. Riera-Palou, “Access point switch on/off strategies for green cell-free massive MIMO networking,” *IEEE Access*, vol. 8, pp. 21788–21803, 2020.
- [15] X. Hu, C. Zhong, X. Chen, W. Xu, H. Lin, and Z. Zhang, “Cell-free massive MIMO systems with low resolution ADCs,” *IEEE Transactions on Communications*, vol. 67, no. 10, pp. 6844–6857, 2019.
- [16] Y. Zhang, M. Zhou, X. Qiao, H. Cao, and L. Yang, “On the performance of cell-free massive MIMO with low-resolution ADCs,” *IEEE Access*, vol. 7, pp. 117968–117977, 2019.
- [17] M. Bashar, K. Cumanan, A. G. Burr, H. Q. Ngo, M. Debbah, and P. Xiao, “Max–min rate of cell-free massive MIMO uplink with optimal uniform quantization,” *IEEE Transactions on Communications*, vol. 67, no. 10, pp. 6796–6815, 2019.

- [18] H. Masoumi and M. J. Emadi, "Performance analysis of cell-free massive MIMO system with limited fronthaul capacity and hardware impairments," *IEEE Transactions on Wireless Communications*, vol. 19, no. 2, pp. 1038–1053, 2019.
- [19] Ö. Özdogan, E. Björnson, and J. Zhang, "Performance of cell-free massive MIMO with Rician fading and phase shifts," *IEEE Transactions on Wireless Communications*, vol. 18, no. 11, pp. 5299–5315, 2019.
- [20] M. Alonzo, S. Buzzi, A. Zappone, and C. DELia, "Energy-efficient power control in cell-free and user-centric massive MIMO at millimeter wave," *IEEE Transactions on Green Communications and Networking*, vol. 3, no. 3, pp. 651–663, 2019.
- [21] F. Rezaei, A. R. Heidarpour, C. Tellambura, and A. Tadaion, "Underlaid spectrum sharing for cell-free massive MIMO-NOMA," *IEEE Communications Letters*, vol. 24, no. 4, pp. 907–911, 2020.
- [22] C. DAndrea, A. Garcia-Rodriguez, G. Geraci, L. G. Giordano, and S. Buzzi, "Analysis of UAV communications in cell-free massive MIMO systems," *IEEE Open Journal of the Communications Society*, vol. 1, pp. 133–147, 2020.
- [23] D. Wang, M. Wang, P. Zhu, J. Li, J. Wang, and X. You, "Performance of network-assisted full-duplex for cell-free massive MIMO," *IEEE Transactions on Communications*, vol. 68, no. 3, pp. 1464–1478, 2019.
- [24] M. Bashar, K. Cumanan, A. G. Burr, H. Q. Ngo, L. Hanzo, and P. Xiao, "On the performance of cell-free massive MIMO relying on adaptive NOMA/OMA mode-switching," *IEEE Transactions on Communications*, vol. 68, no. 2, pp. 792–810, 2019.
- [25] M. Bashar, A. Akbari, K. Cumanan, H. Quoc Ngo, A. G. Burr, P. Xiao, M. Debbah, and J. Kittler, "Exploiting deep learning in limited-fronthaul cell-free massive MIMO uplink," *Early Access in IEEE Journal on Selected Areas in Communications*, 2020.
- [26] Y. Jin, J. Zhang, S. Jin, and B. Ai, "Channel estimation for cell-free mmWave massive MIMO through deep learning," *IEEE Transactions on Vehicular Technology*, vol. 68, no. 10, pp. 10325–10329, 2019.
- [27] S. Mukherjee and J. Lee, "Edge computing-enabled cell-free massive MIMO systems," *IEEE Transactions on Wireless Communications*, vol. 19, no. 4, pp. 2884–2899, 2020.
- [28] H. Xu, N. Huang, Z. Yang, J. Shi, B. Wu, and M. Chen, "Pilot allocation and power control in D2D underlay massive MIMO systems," *IEEE Communications Letters*, vol. 21, no. 1, pp. 112–115, 2016.
- [29] H. Xu, W. Xu, Z. Yang, Y. Pan, J. Shi, and M. Chen, "Energy-efficient resource allocation in D2D underlaid cellular uplinks," *IEEE Communications Letters*, vol. 21, no. 3, pp. 560–563, 2016.
- [30] Z. Yang, N. Huang, H. Xu, Y. Pan, Y. Li, and M. Chen, "Downlink resource allocation and power control for device-to-device communication underlying cellular networks," *IEEE Communications Letters*, vol. 20, no. 7, pp. 1449–1452, 2016.
- [31] A. He, L. Wang, Y. Chen, K.-K. Wong, and M. ElKashlan, "Spectral and energy efficiency of uplink D2D underlaid massive MIMO cellular networks," *IEEE Transactions on Communications*, vol. 65, no. 9, pp. 3780–3793, 2017.
- [32] H. Xu, W. Xu, Z. Yang, J. Shi, and M. Chen, "Pilot reuse among D2D users in D2D underlaid massive MIMO systems," *IEEE Transactions on Vehicular Technology*, vol. 67, no. 1, pp. 467–482, 2017.
- [33] X. Liu, Y. Li, X. Li, L. Xiao, and J. Wang, "Pilot reuse and interference-aided MMSE detection for D2D underlay massive MIMO," *IEEE Transactions on Vehicular Technology*, vol. 66, no. 4, pp. 3116–3130, 2016.
- [34] X. Lin, R. W. Heath, and J. G. Andrews, "The interplay between massive MIMO and underlaid D2D networking," *IEEE*

- Transactions on Wireless Communications*, vol. 14, no. 6, pp. 3337–3351, 2015.
- [35] X. Liu, Y. Li, L. Xiao, and J. Wang, “Performance analysis and power control for multi-antenna V2V underlay massive MIMO,” *IEEE Transactions on Wireless Communications*, vol. 17, no. 7, pp. 4374–4387, 2018.
 - [36] A. Ghazanfari, E. Björnson, and E. G. Larsson, “Optimized power control for massive MIMO with underlaid D2D communications,” *IEEE Transactions on Communications*, vol. 67, no. 4, pp. 2763–2778, 2018.
 - [37] L. Xu, X. Lu, S. Jin, F. Gao, and Y. Zhu, “On the uplink achievable rate of massive MIMO system with low-resolution ADC and RF impairments,” *IEEE Communications Letters*, vol. 23, no. 3, pp. 502–505, 2019.
 - [38] C. Kong, C. Zhong, S. Jin, S. Yang, H. Lin, and Z. Zhang, “Full-duplex massive MIMO relaying systems with low-resolution ADCs,” *IEEE Transactions on Wireless Communications*, vol. 16, no. 8, pp. 5033–5047, 2017.
 - [39] J. Zhang, L. Dai, Z. He, S. Jin, and X. Li, “Performance analysis of mixed-ADC massive MIMO systems over Rician fading channels,” *IEEE Journal on Selected Areas in Communications*, vol. 35, no. 6, pp. 1327–1338, 2017.
 - [40] A. Mezghani and J. A. Nossek, “Capacity lower bound of MIMO channels with output quantization and correlated noise,” in *Proc. IEEE Int. Symp. Inf. Theory*, pp. 1–5, 2012.
 - [41] Y. Zhou and W. Yu, “Fronthaul compression and transmit beamforming optimization for multi-antenna uplink C-RAN,” *IEEE Transactions on Signal Processing*, vol. 64, no. 16, pp. 4138–4151, 2016.
 - [42] T. L. Marzetta, E. G. Larsson, H. Yang, and H. Q. Ngo, *Fundamentals of massive MIMO*. Cambridge University Press, 2016.
 - [43] S. M. Kay, *Fundamentals of statistical signal processing*. Prentice Hall PTR, 1993.
 - [44] X. Zhu, L. Dai, and Z. Wang, “Graph coloring based pilot allocation to mitigate pilot contamination for multi-cell massive MIMO systems,” *IEEE Communications Letters*, vol. 19, no. 10, pp. 1842–1845, 2015.
 - [45] E. Björnson, J. Hoydis, L. Sanguinetti, *et al.*, “Massive MIMO networks: Spectral, energy, and hardware efficiency,” *Foundations and Trends in Signal Processing*, vol. 11, no. 3-4, pp. 154–655, 2017.
 - [46] H. Q. Ngo, E. G. Larsson, and T. L. Marzetta, “Energy and spectral efficiency of very large multiuser MIMO systems,” *IEEE Transactions on Communications*, vol. 61, no. 4, pp. 1436–1449, 2013.